JOURNAL OF MATERIALS SCIENCE **39** (2004) 5799–5801

Investigation on the growth and structure of Fe-doped near-stoichiometric $LiNbO_3$ crystal

T. ZHANG, B. WANG*, S. Q. FANG, Y. Q. ZHAO, F. R. LING, Y. H. XU
Electro-Optics Technology Center, Harbin Institute of Technology, Harbin 150001, People's Republic of China
E-mail: wangbiao@hit.edu.cn
E-mail: tzhang_hit02@yahoo.com

The Fe-doped near-stoichiometric $LiNbO_3$ crystal has been grown from the Li-rich melt by Czochralski method. The UV-Vis absorption spectra, IR transmittance spectra and X-ray diffraction were measured and used to study the defect structure of the crystal. Compared with that of congruent Fe:$LiNbO_3$, in near-stoichiometric Fe:$LiNbO_3$, the lattice parameter reduces, the basal absorption edge shifts towards shorter wavelength, and the OH stretching vibration absorption band shifts towards the lower wavenumber side (3466 cm^{-1}) in the Fe-doped near-stoichiometric $LiNbO_3$.

1. Introduction

Lithium niobate (labeled as $LiNbO_3$, LN) single crystal exhibits excellent electro-optics, ferroelectric, piezoelectric, acoustic and nonlinear properties. These attracting features makes $LiNbO_3$ widely used in second harmonic generation (SHG) [1], holographic storage [2, 3], optical waveguides [4, 5] and fiber sensors [6]. Although nominally pure congruent $LiNbO_3$ crystals (labeled as CLN) generally have good quality and compositional uniformity, a high concentration of intrinsic defects, i.e., Nb_{Li} (Nb occupied Li site) and V_{Li} (Li vacancy) according to Li-site vacancy model [7, 8], are always present in the crystals. The near-stoichiometric $LiNbO_3$ (labeled as SLN) has fewer defects and a better photorefractive ability because of its more ideal structure in crystal ([Li]/[Nb] ≈ 1, atomic ratio). It has been demonstrated that many optical properties of $LiNbO_3$ are related to the [Li]/[Nb] ratio in the crystal, and compositions of the dopants [9, 10]. The effect of Li concentration in crystals on the defect structure of $LiNbO_3$ is still unclear, and the lattice site occupied by impurities ions in $LiNbO_3$ is not universally accepted.

In this paper, we describe the growth of Fe-doped near-stoichiometric $LiNbO_3$ single crystal. The as-grown ferroelectric domain structure, X-ray diffraction, UV-Vis absorption spectra and IR transmittance spectra are measured to investigate the structure and defects of the crystal.

2. Experimental procedure

2.1. Crystal growth

The Fe doped near-stoichiometric $LiNbO_3$ crystal (Fe:SLN) was grown from a Li-rich melt, [Li]/[Nb] = 1.38, by the conventional Czochalski method in air atmosphere. During the growth, the automatic diameter control (ADC) apparatus was not employed because of its low growth rate, 0.3 mm/h. Compared to the actual investigation the two congruent $LiNbO_3$ crystals were also grown. The raw materials for crystal growth are $LiCO_3$, Nb_2O_5, Fe_2O_3 and MgO with the purity of 99.99%. The compositions and doping levels are listed in Table I. A careful preparation of the starting material for the crystal growth is necessary for good quality crystal. So the appropriately weighed materials were thoroughly mixed and calcined at 700°C for 1 h then sintered at 1200°C for 2 h, respectively.

The transparent, crack-free and inclusion-free single crystals were grown along the *c*-axis under optimum growth parameters as listed in Table I. After annealing at 1200°C for 8 h in a furnace where the temperature gradient was almost 5°C/cm, the CLN crystals were polarized with a applied DC electric field of 5 mA/cm^2 for 30 min. While the polarization treatment was not needed for Fe:SLN crystals. Then the crystals were made into samples after being cut, polished. The sample size is listed in Table I. For characterization of the domain structure the 5 mm × 5 mm × 2 mm Z-cut slice from the bulk as-grown No. 3 was cut and polished. In order to reveal the ferroelectric domain structure, the slice was etched in a mixed acid solution ($HF:HNO_3$ = 1:2, volume ratio) at 100°C for 30 min. The etched samples were tested under the optical microscope to determine domain structure. The results obtained show the single domain in the CLN and SLN crystals.

2.2. Characterization

The X-ray powder analyses of the crystals were performed for phase identification and lattice parameters

*Author to whom all correspondence should be addressed.

TABLE I Compositions, doping levels, appearance and growth condition for crystals

Crystals	No. 1	No. 2	No. 3
[Li]/[Nb] starting composition	0.946	0.946	1.38
[Fe_2O_3] (wt%)	0	0.01	0.01
Crystal size (mm)	$\phi 25 \times 30$	$\phi 25 \times 35$	$\phi 15 \times 15$
Sample size (mm^3)	$10 \times 10 \times 3$	$10 \times 10 \times 3$	$10 \times 10 \times 3$
Appearance	Transparent	Transparent	Transparent
Growth temperature (°C)	1250	1250	1180
Temperature gradient (°C/cm)	20	20	40
Pulling rate (mm/h)	2	2	0.3
Seed rotating rate (rpm)	15	15	20

TABLE II The lattice parameter for the crystals. According to Li-site vacancy

Lattice	No. 1	No. 2	No. 3
a (Å)	5.14590	5.14599	5.14261
c (Å)	13.83909	13.83987	13.71938

were determined by a D/max-γB mode X-ray diffractometer with a rotating anode. The measurement conditions were with the wavelength of 1.5405000 Å, copper target and tube voltage/current of 40 kV/50 mA. Calculation of the lattice parameters was carried out on the computer using the least square fitting method, and the data were listed in Table II.

The UV-Vis. absorption spectra of the crystals was recorded by a CARYIE model UV-Vis. spectrophotometer at room temperature. The measurement wavelength range was from 300 to 900 nm. The IR transmittance spectra of the crystals were recorded by a Fourier spectrophotometer with the wavenumber of 3000–4000 cm^{-1} at room temperature.

3. Results and discussions

The X-ray diffraction measurement shows that there is no new peak in the diffraction patterns of Fe:SLN compared with that of pure LN. It shows dopants has entered into the lattice of crystals, exhibiting trigonal structure. But due to the size difference between dopant ions and Li^+, Nb^{5+}, it leads to the change of size and shape in unit cell. So compared with the pure LN, the site and diffraction intensity of peaks is slightly changed.

Table II shows the lattice parameter for the crystals. According to Li-site vacancy model [7, 8], there is a high concentration of intrinsic defects, such as anti-site Nb_{Li} and V_{Li}, in $LiNbO_3$ crystal. In Fe:SLN crystal, more Li ions enter the defect sites of Nb_{Li} and V_{Li}, resulting into the decrease of lattice parameter in unit cell compared with that of Fe:CLN.

The UV-Vis absorption spectra of the crystals are shown in Fig. 1. It is seen that the absorption edge of Fe:SLN shifts to the shorter wavelength compared with that of Fe:CLN, while shifts to the longer wavelength compared with that of the pure LN.

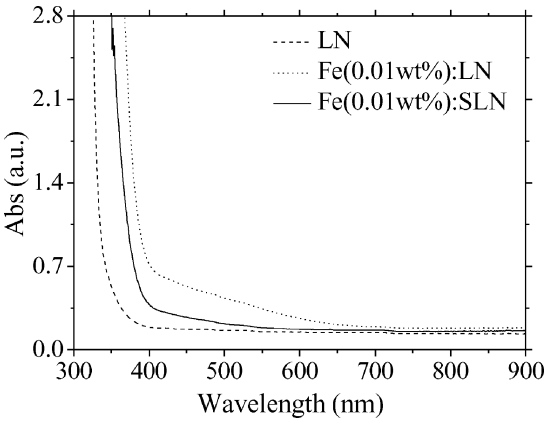

Figure 1 The UV-Vis absorption spectra of the crystals (No. 1–No. 3).

It is well known that the basal absorption transition in $LiNbO_3$ includes the direct transition and the indirect transition [11–14]. The former corresponds to the electrons transition from the valence band (p state of the oxygen ion) vertically to the conduction band (d state of the niobium transition-metal ion) under the action of photons. For the direct transition, the optical absorption coefficient is usually is the order of larger than 10^3 cm^{-1}, and the forbidden energy gap is over 3.8 eV [15]. The indirect transition is composed of the transition absorption related to impurities of defects, absorbing phonons and emitting phonons, respectively. The corresponding optical absorption coefficient is less than the order of 10^3 cm^{-1}, and the forbidden energy gap is near 3.2 eV [15]. When the photon energy exceeds the difference of the indirect transition energy gap and the phonon energy, the absorption of phonons will occur. While the photon energy exceeds the sum of the indirect transition energy gap and the phonon energy, the emission of phonons will take place. The electron energy band structure of $LiNbO_3$ shows the bottom of the conduction band and the top of the valence band are not at the same wavevector K [16]. Therefore, an indirect transition may occur in the optical absorption transition for the doped $LiNbO_3$ crystals.

Fig. 1 shows the indirect transition absorption edge of Fe:SLN exhibits a slight shift to shorter wavelength. The shift of the absorption edge may be explained as follows. According to the theory of Didomenico *el al.* [17], the intensity of the Nb─O band will affect the forbidden band gap. While the valence electronic state of the oxygen ions will affect the position of the indirect transition absorption edge. If the polarization ability of the doped ion in the crystal lattice is higher that of the replaced ion, the interaction of positive and negative ions (doped ion vs. oxygen ion) will result in the electron clouds' distortion level increase of O^{2-}, i.e., the intensity of Nb─O band is weakened and therefore the energy required for the electron transition decrease. Thus the absorption edge shifts towards longer wavelength. Otherwise, it shifts to shorter wavelength. In Fe:SLN crystal, it has less intrinsic defects of Nb_{Li} than in Fe:CLN. This reduces the distortion level of oxygen ions, so the basal optical absorption edge of Fe:SLN shifts to shorter wavelength.

The stoichiometric character of these crystals has manifested in the infrared transmission spectra as well.

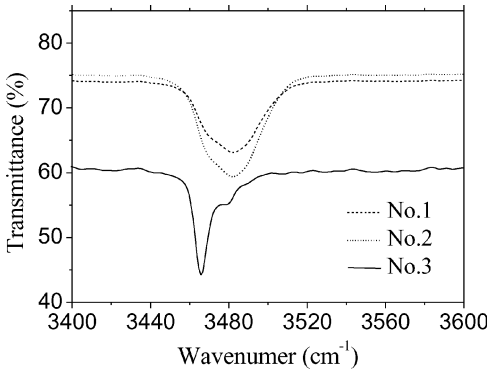

Figure 2 The IR transmittance spectra related to the OH stretching vibration for the crystals.

In Fig. 2 the OH stretching vibration band is shown for the crystals. The pure congruent sample (No. 1) presents a broad non-symmetrical absorption band (FWHM of about 30 cm^{-1}) at approximately 3482 cm^{-1} which has already been observed by Herrington *el al.* [18]. The absorption band of Fe(0.01 wt%):LN (No. 2) is similar to that of pure LN (No. 1). But in Fe(0.01 wt%):SLN (No. 3) the absorption band is shifted to 3466 cm^{-1} which shows a narrow line (FWHM less than 4 cm^{-1}).

It has been reported that the behavior of the OH stretching vibration in $LiNbO_3$ has a strong relationship with the concentration in the crystal and reflects the defect structures [19, 20]. It means that the abrupt IR absorption band is attributed to the change of hydrogen in the oxygen planes of $LiNbO_3$, i.e., the cationic circumstance change. Therefore, the a narrow line at about 3466 cm^{-1} for the IR absorption band can be explained by the smaller amount of defects such as anti-site Nb_{Li} and V_{Li} for Fe:SLN (No. 3) crystal.

4. Conclusions

In conclusions, we have grown the transparent, crack-free and inclusion-free Fe-doped near-stoichiometric $LiNbO_3$ crystal and studied the structure of the crystal by X-ray diffraction, UV-Vis absorption spectra and IR transmittance spectra. The analysis of the results suggests that smaller amount of Nb_{Li} and V_{Li} for Fe(0.01 wt%):SLN result in that the lattice parameter is reduced, the basal absorption edge shifts towards shorter wavelength and the OH stretching vibration absorption band shifts towards the lower wavenumber side (3466 cm^{-1}) in comparison with that of Fe(0.01 wt%):CLN.

Acknowledgements

This work is financially supported by National Research for Fundamental Key Projects No. 973 (G19990330), National Advanced Technology Program No. 863 (2001AA31304), the National Natural Science Foundation (10172030, 50232030), and the Nature Science Foundation of Heilongjiang Province (A01-01), People's Republic of China.

References

1. M. H. LI, Y. H. XU, R. WANG, X. H. ZHEN and C. Z. ZHAO, *Cryst. Res. Technol.* **36** (2002) 191.
2. C.-T. CHEN, D. M. KIM and D. VON DER LINDE, *Appl. Phys. Lett.* **34** (1979) 321.
3. F. MOK, M. TACKITT and H. M. STOLL, *Opt. Soc. Am. Tech. Dig. Ser.* **12** (1989) 74.
4. V. A. FEDOROV, Y. N. KORKISHKO, G. LIFANTE and F. CUSSÓ, *J. Europ. Ceram. Soc.* **19** (1999) 1563.
5. G. LIFANTE, E. CANTELAR, J. A. MUÑOZ, R. NEVADO, J. A. SANZ-GARCÍA and F. CUSSÓ, *Opt. Mater.* **13** (1999) 181.
6. Y. N. KORKISHKO and V. A. FEDOROV, "Ion Exchange in Single Crystals for Integrated Optics and Optoelectronics" (Cambrige International Science Publishing, 1997) p. 490.
7. N. IYI, K. KITAMURA, F. IZUMI, J. K. YAMAMOTO, T. HAYASHI, H. ASANO and S. KIMURA, *J. Solid State Chem.* **101** (1992) 340.
8. N. IYI, K. KITAMURA, Y. YAJIMA and S. KIMURA, *ibid.* **118** (1995) 148.
9. S. C. ABRAHAMS and P. MARSH, *Acta Crystallogr* B **42** (1986) 61.
10. Y. FURUKAWA, M. SATO, K. KITAMURA, Y. YAJINA and M. MINAKATA, *J. Appl. Phys.* **72** (1992) 3250.
11. D. REDFIELD and W. J. BURKE, *ibid.* **45** (1974) 4566.
12. H. A. WEAKLIEM and D. REDFIELD, *RCA. Rev.* **36** (1975) 149.
13. S. M. LI, G. Y. ZHANG, F. RONG, S. J. WU, W. KANG and Q. C. LIU, *Acta Physica Sinica* **34** (1985) 275.
14. S. M. LI, G. Y. ZHANG and J. B. GUO, *ibid.* **35** (1986) 1357.
15. X. L. YANG, G. F. XU, H. P. LI, J. B. ZHU and X. WANG, *J. Sichuan Univ. Sci. Techn.* **19** (2000) 136.
16. S. K. KAM, J. H. HENKEL and H. C. HWANG, *J. Chem. Phys.* **69** (1978) 1949.
17. M. DIDOMENICO and S. H. WEMPLE, *J. Appl. Phys.* **40** (1969) 720.
18. J. R. HERRINGTON, B. DISCHLER, A. RAUBER and J. SCHNEIDER, *Solid State Commun.* **12** (1973) 351.
19. L. KAVACS, M. WOHLECKE, A. JAVANOVIC, K. POLAR and S. KAPPHAN, *J. Phys. Chem. Solids* **52** (1991) 979.
20. Y. WATANABE, T. SOTA, K. SUZUKI, N. IYI, K. KITAMURA and S. KIMURA, *J. Phys.: Condens. Matter* **7** (1997).

Received 16 July 2003
and accepted 29 April 2004